ChemPubSoc Europe

DOI: 10.1002/chem.201503385

CHEMISTRY
A European Journal
Full Paper

Macrocycles

Homodiselenacalix[4]arenes: Molecules with Unique Channelled Crystal Structures

Joice Thomas,[a] Liliana Dobrzańska,[a] Luc Van Meervelt,[b] Mario Alfredo Quevedo,[c] Krzysztof Woźniak,[d] Marcin Stachowicz,[d] Mario Smet,[a] Wouter Maes,[a, e] and Wim Dehaen*[a]

Abstract: A synthetic route towards homodiselenacalix[4]arene macrocycles is presented, based on the dynamic covalent chemistry of diselenides. The calixarene inner rim is decorated with either alkoxy or *tert*-butyl ester groups. Single-crystal X-ray analysis of two THF solvates with methoxy and ethoxy substituents reveals the high similarity of their molecular structures and alterations on the supramolecular level. In both crystal structures, solvent channels are present and differ in both shape and capacity. Furthermore, the methoxy-substituted macrocycle undergoes a single-crystal-to-single-crystal transformation during which the molecular structure changes its conformation from 1,3-alternate (loaded with THF/water) to 1,2-alternate (apohost form). Molecular modelling techniques were applied to explore the conformational and energetic behaviour of the macrocycles.

Introduction

There is a continuing demand for new, easy-to-synthesise, organic materials that form channels or voids in the crystalline phase. Examples of these molecules include resorcinarene derivatives,[1a] tris-(*o*-phenylenedioxy)cyclotriphosphazene,[1b] cucurbit[6]uril,[1c] bisurea macrocycles,[1d] some chalcogen-containing cyclic alkynes and alkenes[1e] and dipeptide crystals.[1f] These materials have drawn attention in the fields of chemical and material sciences for gas storage and selective gas recognition and separation. There is also a growing interest in crystalline materials with so-called dynamic pores that respond to guest uptake/removal without crystal disintegration.[2] However, these are still rarely encountered among organic compounds.[3,12] The main driving forces for the formation of supramolecular organic frameworks are the geometrical constraints on the building blocks, which favour a particular molecular conformation achieved through a net of different supramolecular interactions, such as hydrogen and halogen bonding and π–π stacking. In the case of soft supramolecular frameworks, these can switch when triggered by external stimuli, which causes reorganisation of the molecules in the crystal unit.

Calix[*n*]arene macrocycles have also received great attention as potentially porous materials. Their molecular cavities in combination with a broad range of functional groups render them excellent candidates for this purpose.[5] One of the most appealing aspects of calixarenes is their availability and susceptibility to chemical modification by ligating groups at both the *endo*- and *exo*-positions of the central annulus. These substituents enable calixarenes to exist in different conformations depending on the rotation around the Ar-CH_2-Ar bonds, which results in the most energetically favourable arrangement of the molecules. The strong interest in the supramolecular chemistry of calixarenes has stimulated efforts to synthesise a number of related macrocycles, such as heteracalix[*n*]arenes,[6,7] homocalix[*n*]arenes[8] and homoheteracalix[*n*]arenes.[8–11] Of the various known "calixarenoid" macro-rings, the supramolecular features of homoheteracalix[*n*]arenes are particularly attractive because they introduce dimethylenehetera linkages and thus provide an additional opportunity to tune the ring size, conformation and binding properties.

The chemistry of homoheteracalixarenes is still relatively under-developed and our search for related receptors by combining our earlier knowledge on heteracalix[*n*]arenes[7] and homoheteracalix[*n*]arenes,[11a,b,12] resulted in the development of a new class of macrocycles called homodithiacalix[4]arenes.[4] They are expanded analogues of homoheteracalix[*n*]arenes in

[a] *Dr. J. Thomas, Dr. L. Dobrzańska, Prof. M. Smet, Prof. W. Maes, Prof. W. Dehaen*
Molecular Design and Synthesis, Department of Chemistry
KU Leuven, Celestijnenlaan 200F, B-3001 Heverlee (Belgium)
E-mail: wim.dehaen@chem.kuleuven.be

[b] *Prof. L. Van Meervelt*
Biomolecular Architecture, Department of Chemistry
KU Leuven, Celestijnenlaan 200F, B-3001 Heverlee (Belgium)

[c] *Prof. M. A. Quevedo*
Unidad de Investigación y Desarrollo en Tecnología Farmacéutica
CONICET. Departamento de Farmacia, Universidad Nacional de Córdoba
Córdoba (Argentina)

[d] *K. Woźniak, M. Stachowicz*
Department of Chemistry, Warsaw University
Pasteura 1, 02-093 Warsaw (Poland)

[e] *Prof. W. Maes*
Design and Synthesis of Organic Semiconductors (DSOS)
Institute for Materials Research (IMO-IMOMEC), Hasselt University
Agoralaan 1 - Building D, 3590 Diepenbeek (Belgium)

Supporting information for this article is available on the WWW under http://dx.doi.org/10.1002/chem.201503385.

which all of the methylene bridges between the aromatic units of the classical calixarenes are replaced by CH_2-S-S-CH_2 groups. As a consequence of the additional heteroatom in the bridge, the homodithiacalix[4]arene macrocycle possesses a higher conformational flexibility compared with the related homothiacalix[4]arenes.[11a] Moreover, it was shown that its THF solvate exhibits a very special solid-state phenomenon, namely, a reversible conformational switching between 1,3-alternate and 1,2-alternate forms in single crystals as a response to solvent uptake/removal. In the single-crystal state, the molecules shift in a concerted fashion and the process is correlated with the formation/disappearance of channels in the structure.[4a]

Thermodynamically controlled dynamic covalent chemistry (DCC) based on disulfide bonds has been used successfully for the synthesis of homodithiacalix[4]arenes and is considered an attractive approach to prepare a range of macromolecules.[13] To date, there has been no report on the selective synthesis of macrocycles by using DCC of diselenide bonds.[14] Glutathione peroxidase (GPx) is an antioxidant enzyme that has a diselenide at its active site and protects various organisms from oxidative damage.[15] Other selenoenzymes that contain selenium in their active sites are iodothyronine deiodinase and thioredoxin reductase.[16] Recently, selenide- and diselenide-containing polymers have been effectively used to develop sensitive responsive systems.[17] Macrocycles containing selenium as a donor atom within the cycle are better σ-donor ligands and show unique coordination behaviour compared with their lighter congeners.[18] Finally, one of the major advantages of Se-based macrocycles is the possibility of monitoring the host–guest interactions by the shift in the ^{77}Se NMR signal.

From the above-mentioned facts, it is evident that calixarenes with CH_2-Se-Se-CH_2 bridges between the aromatic units of the macrocyclic framework are attractive target molecules in diverse domains of supramolecular chemistry. Herein, we report a successful DCC approach for the synthesis of homodiselenacalix[4]arenes, the covalent synthesis of which has not been explored to date. The solution chemistry is supported by single-crystal X-ray studies and molecular modelling.

Results and Discussion

Synthesis and Characterisation

The extremely simple and high-yield synthetic procedure, together with the remarkable supramolecular features of the homodithiacalix[4]arene macrocycle in the solid state,[4] encouraged us to use an analogous building block for the generation of bis-selenolate anions. Diselenol derivatives are, however, not easy to prepare and difficult to handle. The required selenium bisnucleophile was thus generated through the reduction of 1,3-bis(selenocyanato)benzene derivative **1** by using $NaBH_4$ as the reducing agent. The first experiment towards the synthesis of homodiselenacalix[*n*]arene macrocycles involved a [2+2] homocoupling reaction by initial reduction of precursor **1** with $NaBH_4$, followed by oxidation in air over a time period of 12 h, to give homodiselenacalix[4]arene **4** as the only macrocyclic product in the reaction mixture (Table 1, entry 1). The tetrameric macrocycle was effectively purified by precipitation in a methanol/water mixture and obtained in a nearly quantitative yield (≥96%) by the concomitant formation of four reversible covalent diselenide bonds. Complete conversion of building block **1** to the macrocycle happens very fast because selenocyanates and the derived selenolates possess an extremely high propensity to produce diselenides (as compared with the conversion of thiocyanates to disulfides). The trimeric and pentameric macrocycles were also observed by using ESI-MS in the beginning of the experiment. However, the reversible nature of the reaction causes the complete conversion of all macrocycles to the thermodynamically more stable homodiselenacalix[4]arene. An effort to isolate the trimeric and pentameric products by quenching the reaction after 1 h was not successful because of difficulties encountered during purification by using column chromatography. The reaction was also repeated on a larger scale (2.5 mmol) and once more complete conversion of the building block to macrocycle **4** (92%) was observed. High-dilution conditions were not necessary for the successful formation of the homodiselenacalix[4]arene.

Table 1. Optimisation of the yield for homodiselenacalix[4]arene **4**.[a]

Entry	Solvent	Reagent(s)	Yield [%][b]
1	THF/EtOH	$NaBH_4$	≥96
2	THF/EtOH	$LiBH_4$	93
3	THF/EtOH	Li	≥95
4	THF/EtOH	Na	92
5	THF/EtOH	K	90
6	THF	BH_3·THF	76
7	THF/EtOH	BH_3·THF/NaI	83
8	THF/EtOH	BH_3·THF/KI	93
9	THF/EtOH	$NaBH_4$/15-crown-5 (1:1)	≥95
10	THF/EtOH	$NaBH_4$/15-crown-5 (1:4)	≥95
11	THF/EtOH	$(n\text{Bu})_4BH_4$	75

[a] Reaction conditions: **1** (0.5 mmol), $NaBH_4$ (1.05 mmol), T=25 °C, solvent EtOH/THF (1:3), and reaction time 12 h. [b] Isolated yield.

After the initial success, a systematic investigation of the effect of different metal ions on the selective formation of macrocycle **4** was conducted (Table 1). A change in the reducing agent from $NaBH_4$ to $LiBH_4$ caused only a marginal difference in the isolated yield of the calixarene (93%; Table 1, entry 2). The yield of **4** also remained nearly quantitative when the reaction was performed with different alkali metals in ethanol/THF (Table 1, entries 3–5). On performing the reaction with the BH_3·THF complex as the reducing agent, the yield of the tetrameric product decreased to 76% (Table 1, entry 6). ESI-MS analysis of the remaining mixture indicated the presence of trimeric and pentameric homodiselenacalix[*n*]arenes, but these macrocycles could not be purified efficiently. To study the influence of Na^+ and K^+ on the selective formation of the homodiselenacalix[4]arene, two separate experiments were conducted with BH_3·THF as the reducing agent in the presence of NaI or KI salts (Table 1, entries 7, 8). In these cases, the amount of homodiselenacalix[4]arene obtained was estimated to be 7 (NaI) and 17% (KI) higher than in the case in which no alkali metal salts were added. However, because these results cannot con-

vincingly prove a possible templating effect of the alkali metal ions, another reaction was performed by using a combination of $NaBH_4$ and 15-crown-5 (1:1 ratio) under the optimised conditions (Table 1, entry 9). The yield of tetrameric macrocycle **4** remained almost quantitative and an increase in the ratio of the Na-complexing crown compound did not decrease the yield of tetrameric macrocycle **4** (Table 1, entry 10). When the reaction was repeated with $(n\text{Bu})_4BH_4$ under the optimised conditions, cyclotetramer **4** was obtained in 75% yield (Table 1, entry 11).

The above experiments indicate that the alkali metal ions do not play a crucial role in facilitating the formation of the tetrameric macrocycle. The crucial parameter to obtain homodiselenacalix[4]arene **4** in high yield and selectivity is the fact that the tetrameric macrocycle is the thermodynamically most stable product, combined with the high reversibility of the Se–Se bond formation. It is worth mentioning again that the inconvenient high-dilution conditions are not required for the successful formation of the homodiselenacalix[4]arene.

To elucidate the mechanism of the reaction that leads to homodiselenacalix[4]arene **4**, we examined the gel permeation chromatography (GPC) profile of the macrocyclic reaction as a function of time (Figure 1). Even after a reaction time of

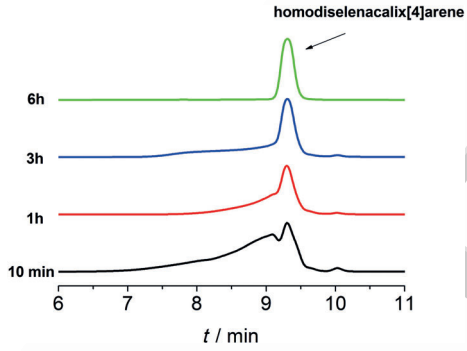

Figure 1. GPC profiles of the macrocyclic reaction that leads to the formation of homodiselenacalix[4]arene **4** as a function of time.

10 min, a substantial amount of calixarene **4** was already observed together with oligomers/polymers with a broad molecular weight distribution. The retention time for the polymers or higher oligomers was observed between 6.2 and 9.2 min, whereas the tetrameric cyclophane was observed at 9.3 min. An increase in the ratio of homodiselenacalix[4]arene **4** together with a subsequent decrease in the polymer content was clearly observed over time. The conversion of polymers to calix[4]arene is fast at the start of the reaction and complete conversion to the tetrameric macrocycle was observed after 6 h. This observation reveals that the building blocks constantly exchange with reversible covalent diselenide bonds, which gives various products with higher preference for the cyclic tetramers over the other cyclic oligomers or polymers. Later, the polymers or other cyclic oligomers undergo fragmentation of the dynamic diselenide bonds into smaller oligomeric units, followed by their recombination to give the thermodynamically most stable products, in this case apparently homodiselenacalix[4]arene **4**. This fragmentation/(re)cyclisation of the building blocks is the major reversible process during the course of the reaction.

To modulate the size of the homodiselenacalix[4]arene cavity and to modify its supramolecular features (in the solid state), different functional moieties can be introduced on the building blocks prior to macrocyclisation. As a proof of concept, the methoxy group was replaced by ethoxy and $OCH_2COO\text{t}Bu$ entities at the intra-annular position of the bis-selenocyanate building block. Under the optimised conditions, the reaction (for 12 h) of bis-selenocyanates **2** and **3** with $NaBH_4$ resulted in the formation of homodiselenacalixarenes **5** and **6** in 89 and 77% yield, respectively (Scheme 1). Similarly

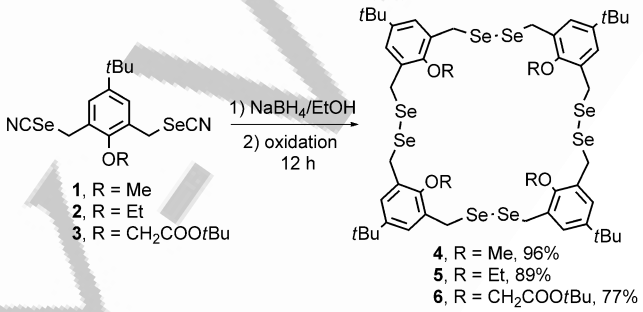

Scheme 1. Synthetic protocol for homodiselenacalix[4]arenes **4**–**6**.

to compound **4**, the trimers and pentamers were initially observed in the reaction mixtures by using ESI-MS, but the reversibility of the cyclisation process gradually converted all these macrocycles into the more stable tetrameric analogues. None of the larger or smaller cyclic oligomers were detected in the reaction mixtures after 12 h.

The ^1H NMR spectrum of homodiselenacalix[4]arene **4** shows a trend similar to that observed for the corresponding homodithiacalix[4]arene,[4] but the intra-annular methoxy groups are slightly more de-shielded for the Se analogue. The large size of Se leads to an increased cavity size and imposes a significant difference on the electronic and conformational features. Homodiselenacalix[4]arene **6**, with four inner-rim *tert*-butyl acetate groups, does not display any geminal coupling for the bridging CH_2 protons (observed previously in the case of di- and tetra-substituted homothiacalix[4]arenes[11a]), which confirms the conformational flexibility of the macrocycles.

Solid-State Structures and Conformational Single-Crystal-to-Single-Crystal (SC–SC) Transformation

Single crystals suitable for X-ray diffraction (XRD) studies were grown for homodiselenacalix[4]arenes **4** and **5** by slow evaporation from THF solutions. Compound **4** (Figure 2) is isostructural with the homodithiacalix[4]arene presented previously.[4] It adopts a 1,3-alternate conformation with all the methoxy groups pointing outside of the cavity. The latter is also apparent from the shift observed for the methoxy protons in the

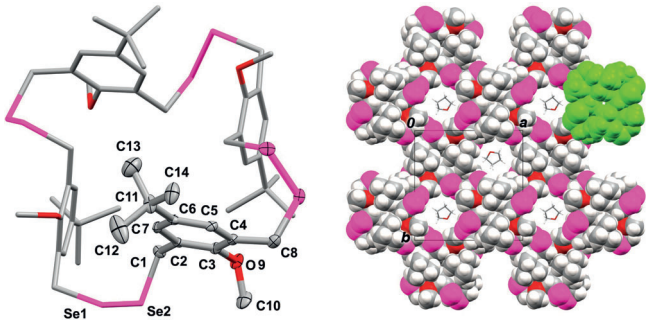

Figure 2. Left: Molecular structure of homodiselenacalix[4]arene **4**; H atoms and solvent molecules are omitted for clarity, displacement ellipsoids (drawn at the 50% probability level) and labelling scheme indicate the asymmetric unit. Right: Packing diagram of homodiselenacalix[4]arene **4**, which shows the formation of channels along the *c* axis; solvent disorder omitted for clarity, one calixarene molecule shown in green.

^{1}H NMR spectrum ($\delta = 3.71$ ppm) in solution. The planes defined by opposite benzene rings are almost parallel to each other (the dihedral angle is 11.6°) with separations between the centroids equal to 7.54 Å, almost the same as in the disulfide analogue (9.5° and 7.55 Å). The macrocyclic ring is strongly folded with methylene groups pointing alternately into and out of the cavity, which is facilitated by intramolecular interactions (Table S1 in the Supporting Information). The calixarene molecules form a 3D supramolecular framework, which results from weak intermolecular C–H···Se hydrogen bonding, namely, C10–H10B·· Se1^{i} (with C···Se = 3.832(7) Å and C-H-Se = 151°, symmetry code i) $1-x$, $-1/2+y$, $z-1/2$) and C8–H8B···Se2^{ii} (with C···Se = 3.957(7) Å and C-H-Se = 158°, symmetry code ii) $-1/2+y$, $1-x$, $1/2+z$), in which solvent channels are present along the *c* axis. The THF molecules filling these pores are weakly associated with the methoxy groups of the host through the O atoms (Table S1 in the Supporting Information).

Comparison of the packing features of macrocycle **4** and its disulfide analogue indicates a slightly larger size of the channels that accommodate the THF molecules in the homodiselenacalixarene, with centroid-to-centroid separations between opposite benzene rings of 10.98 Å (10.56 Å for the compound with S–S) and 9.28 Å between adjacent rings (9.05 Å for the S–S analogue). The fact that molecule **4** is isostructural with the crystal structure of the previously reported homodithiacalix[4]-arene encouraged us to check whether this compound is also able to undergo a conformational transformation upon solvent removal. The experiment was successful and we were able once again to monitor the transformation of the 1,3-alternate form to 1,2-alternate (**4a**) by using single-crystal XRD, after heating a crystal at 155 °C for 3 min (Figure 3; for an overlay, see Figure S1 in the Supporting Information). The transformation was also followed by X-ray powder diffraction (XRPD) studies performed for a range of temperatures (30–150 °C; Figures S4–S6 in the Supporting Information). It was shown that at 100 °C all molecules of **4** are transformed to **4a**. This means that after solvent removal, which is takes place at around 110 °C (as shown by thermogravimetric analysis (TGA), Figure S7 in the Supporting Information), all molecules are being

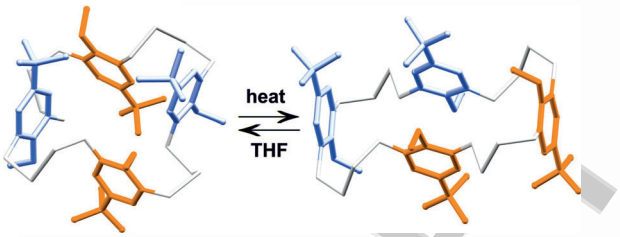

Figure 3. Representation of the transformation that takes place in the single crystal upon solvent removal/uptake (H atoms omitted for clarity).

converted to **4a**.[19] Structure **4a** is reminiscent of the 1,2-alternate form of the disulfide analogue. The molecules in **4a** are densely packed, which means that no channels are present in the crystal structure and new supramolecular interactions are established. In the disulfide congener, the molecules are held together by intermolecular weak C–H···Se interactions forming layers in the *ac* plane (Table S1 in the Supporting Information), further stabilised by C13–H13B···Cg^{i} contacts with a C···Cg contact of 3.706(3) Å (Cg is the centroid of the ring C2–C7, symmetry operation: i) $1-x$, $1-y$, $-z$), which expands the layers in the third dimension.

Comparison of the centroid-to-centroid separation between opposite phenyl rings in macrocycles **4** (7.54 Å) and **4a** (3.97 and 12.09 Å) reveals once again significant shrinkage/expansion of the molecules. The fact that the crystals survive such a drastic transformation, which involves rotation of the aryl rings and reorientation of the methoxy groups, is again astonishing.[4a]

The molecular structure of homodiselenacalix[4]arene **5** (Figure 4), with an ethoxy group at the intra-annular positions, exhibits a 1,3-alternate conformation similar to **4**. In fact, the molecular structures of **4** and **5** are almost identical (Figure 4). The supramolecular assemblies formed, however, differ to a large extent. Compound **5** crystallises in the space group *C*2/*c* with half of a calixarene molecule and one THF molecule in the asymmetric unit (Figure 5). The *tert*-butyl groups are disordered over two sites, with occupancy factors 0.71(1) and 0.29(1) for the one that contains C10 and 0.62(1) and 0.38(1)

Figure 4. Superposition of macrocycles **4** (green) and **5** (red).

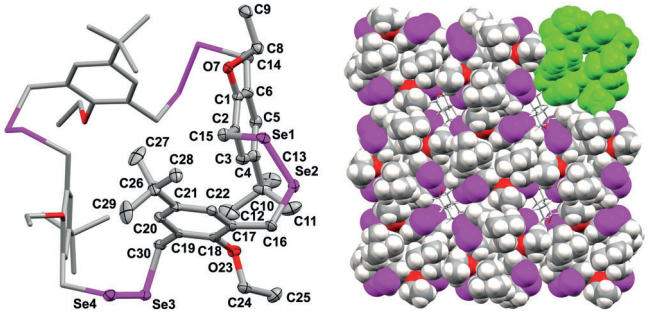

Figure 5. Left: Molecular structure of homodiselenacalix[4]arene **5**; H atoms and solvent molecules omitted for clarity, displacement ellipsoids (drawn at the 50% probability level) and labelling scheme indicate the asymmetric unit. Right: Packing diagram of **5** in space-filling representation shown along the *b* axis; disorder on *tert*-butyl groups C10 and C26 omitted for clarity, one calixarene molecule shown in green.

for the one with C26. The separations between the centroids of opposite phenyl rings in the macrocycle are 7.87 and 7.52 Å, which shows an increase of approximately 0.3 Å in one pair of rings compared with **4**. The dihedral angles between these semi-parallel aromatic rings are 13.7 and 10.8°, respectively. The host molecules pack with the formation of solvent channels (along the *b* axis in this case) in which the guest molecules are being surrounded by the Se2 and Se4 atoms and CH_2 groups from adjacent macrocycles. Contrary to **4**, the alkoxy substituents and *tert*-butyl groups do not border these apertures. The channels in **5** are zig-zag shaped and have a smaller capacity than in **4** (Figure S3 in the Supporting Information). Moreover, in the former the guests interact more strongly with the host. This is evident from the geometrical hydrogen-bonding parameters C16–H16B···O33 (O33 originates from THF, C···O is 3.326(10) Å and C-H-O = 157°). Additionally, there is a weaker contact, namely, C35–H35A···Se2^{i} (C35–H35A originates from THF, C···Se = 3.929(11) Å and C-H-Se = 148°, symmetry code i) 1/2−*x*, −1/2+*y*, 3/2−*z*).

The hydrogen bonds present between the host and guest molecules lead to the formation of 2D layers in the *ab* plane, which are interconnected in the third dimension by very weak intermolecular C25–H25C···Se4^{ii} (C–Se = 3.600(8) Å, C-H-Se = 111°, symmetry code ii) −*x*, 2−*y*, 1−*z*) contacts. Attempts to empty the channels present in **5** failed. It seems that removal of the solvent molecules, which interact much more strongly with the host, initiates decomposition of the material.

Molecular Modelling Studies

To study the structural features of the homodiselenacalix[*n*]arenes that contain three, four and five subunits, the corresponding structures were constructed and afterwards subjected to exhaustive molecular modelling studies. These studies aimed to identify a quantitative basis to support the enhanced stability observed for the homodiselenacalix[4]arenes with respect to the smaller (calix[3]arene) and larger (calix[5]arene) ring systems, as observed experimentally.

The lowest energy conformation for each molecule is required to start structural analyses. Thus, simulated annealing procedures were performed for the three macrocycles. The conformations corresponding to the minimum energies are shown in Figure S8 in the Supporting Information, in which it can be seen that **4** exhibits a distorted 1,3-alternate conformation. In addition, the homodiselenacalix[3]arene exhibits a conformation in which one methoxy and two *tert*-butyl moieties are oriented towards the same direction in the macrocycle, whereas the homodiselenacalix[5]arene has a much higher molecular flexibility, with one of the subunits positioning its methoxy substituent inside the macrocyclic cavity. The whole set of simulated annealing runs ($n = 20$) converged to the above-described molecular conformations, and these were thus considered as the minimum-energy conformations and used as initial coordinates for the following molecular dynamics (MD) analyses.

Molecular dynamics simulations were again performed for the corresponding macrocycles with three, four and five subunits, under both implicit and explicit solvent conditions and simulated at 300 K for 10 ns. For analyses performed under implicit solvent conditions, a dielectric constant of 7.6 was used to simulate a THF environment at 300 K. Convergence plots of the resulting trajectories were constructed and analysed from the corresponding root-mean-square deviation (rmsd) versus time plots (Figure S9 in the Supporting Information). As can be seen, the structures of the macrocycles formed by three and five units reached stable structures at the beginning of the simulation and remained stable up to the last 10 ns of the trajectory. Conversely, the structure corresponding to homodiselenacalix[4]arene **4** alternated between two clusters of conformations; the first cluster of conformations existed in the time frames within snapshots 5000 to 22000 and 82000 to 92000, whereas the second cluster of conformations was present in the range of 30000 to 80000. As shown by the trajectory analysed over 10 ns, the reconversion between these two clusters of conformations is energetically feasible under the simulated conditions.

To quantitatively assess the stability of the homodiselenacalixarene macrocycles, the total energy (E_{TOT}), potential energy (E_{PTOT}) and kinetic energy (E_{KTOT}), as calculated from the force field applied during the MD study, were compared (Figure S10 in the Supporting Information, Table 2).

As can be seen, the macrocycle with four units exhibits a lower E_{TOT} value (33.21 kcal mol^{-1}), which suggests it has higher stability than the calixarenes with three or five subunits (78.01 and 71.52 kcal mol^{-1}, respectively). This observation is consistent with the experimental observations that show that

Table 2. Total energy (E_{TOT}), potential energy (E_{PTOT}) and kinetic energy (E_{KTOT}) values calculated for homodiselenacalix[*n*]arene macrocycles with three, four and five subunits.

Subunits	*E* [kcal mol^{-1}]		
	E_{TOT}	E_{PTOT}	E_{KTOT}
3	78.01 (±0.06)	−13.22 (±0.05)	91.24 (±0.04)
4	33.21 (±0.08)	−88.43 (±0.05)	121.64 (±0.05)
5	71.52 (±0.08)	−80.61 (±0.06)	152.12 (±0.06)

the homodiselenacalixarenes containing three and five subunits are initially detected in the reaction media, but are readily converted to the homodiselenacalix[4]arene macrocycle as the synthetic reaction proceeds. Further inspection of Figure S10 in the Supporting Information revealed that the stabilisation of the macrocycle with four subunits originates in a lower-than-expected E_{PTOT}, which results in a lower E_{TOT} when combined with a favourable balance with the corresponding E_{KTOT}. To assess the structural features at the base of the above-mentioned energetic behaviour, the E_{PTOT} value was further decomposed in the corresponding energy terms: E_{BOND}, E_{ANGLE}, E_{DIHED}, E_{VDW}, E_{ELE}, E_{EGB}, E_{1-4ELE} and E_{1-4VDW} (Figure S11 in the Supporting Information and Table 3).

Table 3. Energetic components included in the potential energy (E_{PTOT}) calculated by using the molecular dynamics force field for homodiselenacalix[*n*]arenes with three, four and five subunits.

Subunits	E [kcal mol^{-1}]							
	E_{BOND}	E_{ANGLE}	E_{DIHED}	E_{VDW}	E_{ELE}	E_{EGB}	E_{1-4ELE}	E_{1-4VDW}
3	36.40 (±0.03)	45.54 (±0.03)	28.45 (±0.02)	−17.28 (±0.02)	−161.55 (±0.09)	−13.95 (±0.07)	41.9 (±0.02)	27.26 (±0.01)
4	48.27 (±0.04)	61.30 (±0.04)	35.39 (±0.02)	−25.89 (±0.02)	−280.06 (±0.12)	−18.76 (±0.10)	55.00 (±0.02)	36.31 (±0.01)
5	60.75 (±0.04)	76.68 (±0.04)	44.23 (±0.02)	−35.80 (±0.02)	−410.74 (±0.19)	−18.61 (±0.16)	157.37 (±0.01)	45.52 (±0.01)

From inspection of Figure S11 in the Supporting Information, a close relationship between the potential energy components for the different homodiselenacalixarenes is observed as an additional subunit is added to the macrocycle. An exception to this feature is found for the E_{1-4ELE} energetic component, which exhibits almost no difference between the macrocycles containing three and four units, and a considerably higher value for the homodiselenacalix[5]arene. This observation results in a lower than expected E_{1-4ELE} component for the homodiselenacalix[4]arene. Taking into account that the E_{1-4ELE} component derives from the intramolecular electrostatic stabilisation between atoms separated by more than three bonds (i.e., a dihedral angle), the lower E_{1-4ELE} found suggests that homodiselenacalix[4]arene is able to adopt a conformation in which a higher electrostatic stabilisation by distant atoms is geometrically favoured.

To investigate the effect of explicit solvent molecules on the conformational and energetic behaviour of compound **4**, MD studies were performed by applying an explicit THF box under periodic solvent conditions. Because no pre-equilibrated THF solvent models are available in the AMBER software package, a model was developed and validated in-house (see technical details in the Experimental Section). After the corresponding solvent box was constructed, parameterised and pre-equilibrated at 300 K, the corresponding density was monitored for a 10 ns trajectory simulation. The results are depicted in Figure S12 in the Supporting Information, in which it can be seen that the calculated density quickly reached the experimental reference value (i.e., 0.889 g cm^{-3}) and remained stable throughout the simulated trajectory.

Production MD runs were performed for the methoxy-substituted homodiselenacalix[*n*]arenes with three, four and five subunits in a THF box under periodic boundary conditions. In addition to standard values for the total, potential and kinetic energies (data not shown), the densities of the solvated systems were monitored as a quality check of the corresponding trajectories (Figure S13 in the Supporting Information), and it was found that all the trajectories were adequately equilibrated and rapidly reached densities of around 0.9 g mL^{-1}. To compare the conformational stabilities of the homodiselenacalix[3]-, calix[4]- and calix[5]arenes, the calculated potential energies of the corresponding systems were again decomposed into the corresponding energetic components (Table 4).

As can be seen in Table 4, the homodiselenacalix[4]arene shows a lower E_{1-4ELE} value (−383.47 kcal mol^{-1}) than its three- and five-membered counterparts (−367.10 and −369.97 kcal mol^{-1}, respectively). Again, explicit solvent MD simulations predict a higher stability for the calix[4]arene compared with the calix[3]arene and calix[5]arene. From analyses of RMSD versus time profiles (Figure S14 in the Supporting Information), it is again observed that the homodiselenacalix[4]arene exists in two clusters of conformations, whereas the calix[3]arene and calix[5]arene maintain a relatively stable conformation during the simulated trajectory. It is also worth noting that the calix[4]arene gains a higher stabilisation derived from E_{1-4ELE} compared with the three- and five-membered macrocycles when explicit THF molecules are present.

Table 4. Energetic components originating from the potential energy (E_{PTOT}) obtained from explicit solvent (THF) molecular dynamics simulations for the homodiselenacalix[*n*]arenes with three, four and five subunits.

Subunits	E [kcal mol^{-1}]						
	E_{BOND}	E_{ANGLE}	E_{DIHED}	E_{VDW}	E_{ELE}	E_{-4ELE}	E_{1-4VDW}
3	303.00 (±13.57)	1666.39 (±30.19)	1525.06 (±16.11)	−1448.70 (±14.89)	114.25 (±7.31)	−367.10 (±2.93)	82.71 (±3.33)
4	330.51 (±14.26)	1803.25 (±31.54)	1645.70 (±16.84)	−1574.75 (±15.38)	13.57 (±7.98)	−383.47 (±4.15)	96.15 (±3.58)
5	397.65 (±15.62)	2163.00 (±34.41)	1972.96 (±18.43)	−1892.60 (±16.82)	−52.49 (±8.79)	−369.97 (±5.07)	116.65 (±3.92)

Overall, the above-presented molecular modelling studies demonstrate that homodiselenacalix[4]arene is energetically favoured over its smaller and larger counterparts due to a more efficient intramolecular electrostatic interaction, which is derived from its dynamic geometric features.

Conclusion

A low-cost and efficient synthetic pathway towards homodiheteracalix[*n*]arenes with bridging CH_2-Se-Se-CH_2 groups between the aryl parts has been established. To the best of our knowledge, this is the first example that applies the dynamic

covalent chemistry of diselenide bonds for the selective synthesis of macrocycles. By using the optimised conditions, homodiselenacalixarene macrocycles with alkoxy groups at the intra-annular positions were synthesised with complete selectivity for the tetrameric macrocycles. The procedure could easily also be extended to a lower-rim *tert*-butyl ester-functionalised homodiheteracalix[4]arene. An important advantage of the presented synthetic procedure is the ease of purification, achieved simply by precipitating the calixarene from the reaction mixture in water and methanol. The macrocycles were completely characterised, including single-crystal X-ray analyses. These studies revealed almost identical molecular structures yet different packing forces for the methoxy- and ethoxy-decorated cyclo-tetramers, which resulted in the formation of one-dimensional channels of various shapes and capacity in both crystal structures. Furthermore, the methoxy-substituted homodiselenacalix[4]arene is able to undergo a SC–SC transformation to give the 1,2-alternate form upon THF/H_2O removal, a process that is reversible. We envision that further studies on this family of compounds based on the modification of functional groups and crystallisation conditions could lead to novel materials with fascinating supramolecular properties (e.g., sorption, sensing and molecular trapping). This is currently under investigation.

Experimental Section

Synthesis of Homodiselenacalix[4]arene Macrocycles

A solution of $NaBH_4$ (40 mg, 1.05 mmol) in ethanol (10 mL) was added dropwise to a solution of precursor **1**, **2** or **3** (0.5 mmol) in THF (30 mL) over 1 h at RT. After stirring the resulting mixture for another 12 h, the reaction mixture was added to a 1:1 mixture of water and methanol (80 mL) and the precipitate that formed was filtered off and dried in vacuum to afford analytically pure products **4**, **5** or **6** as off-white solids.

Homodiselenacalix[4]arene (4)

Yield: 96% (168 mg); m.p. 185–186 °C; ^{1}H NMR (300 MHz, $CDCl_3$): $\delta = 7.00$ (s, 8H), 3.80 (s, 16H), 3.71 (s, 12H), 1.25 ppm (s, 36H); ^{13}C NMR (75 MHz, $CDCl_3$): $\delta = 153.8$, 146.8, 131.9, 127.3, 62.3, 34.4, 31.6, 28.1 ppm; ^{77}Se NMR (76.3 MHz, $CDCl_3$): $\delta = 403$ ppm; HRMS (ESI^+): *m/z* calcd for $C_{52}H_{72}O_4Se_8$: 1422.8642 $[M+Na]^+$; found: 1422.8649.

Homodiselenacalix[4]arene (5)

Yield: 89% (161 mg); m.p. 105–106 °C; ^{1}H NMR (300 MHz, $CDCl_3$): $\delta = 6.91$ (s, 8H), 4.01 (q, $J = 6.7$ Hz, 8H), 3.55 (s, 16H), 1.38 (t, $J = 6.7$ Hz, 12H), 1.25 ppm (s, 36H); ^{13}C NMR (100 MHz, $CDCl_3$): $\delta =$ 152.5, 145.6, 131.8, 127.4, 69.7, 34.2, 31.6, 26.8, 16.1 ppm; ^{77}Se NMR (76.3 MHz, $CDCl_3$): $\delta = 399$ ppm; HRMS (ESI^+): *m/z* calcd for $C_{56}H_{80}O_4Se_8$: 1478.9268 $[M+Na]^+$; found: 1478.9259.

Homodiselenacalix[4]arene (6)

Yield: 77% (173 mg); m.p. 78–79 °C; ^{1}H NMR (300 MHz, $CDCl_3$): $\delta =$ 7.13 (s, 8H), 4.53 (s, 8H), 4.10 (s, 16H), 1.50 (s, 36H), 1.29 ppm (s, 36H); ^{13}C NMR (100 MHz, $CDCl_3$): $\delta = 168.3$, 152.7, 147.2, 132.2, 127.3, 82.3, 71.8, 34.4, 31.6, 28.4 ppm; ^{77}Se NMR (76.3 MHz, $CDCl_3$): $\delta = 385$ ppm; HRMS (ESI^+): *m/z* calcd for $C_{72}H_{104}O_{12}Se_8$: 1823.0739 $[M+Na]^+$; found: 1823.0695.

Crystallographic Data

Single-crystal X-ray diffraction data for compounds **4** and **5** were collected by using a Bruker SMART 6000 diffractometer equipped with a CCD detector and by using $Cu_{K\alpha}$ radiation ($\lambda = 1.54178$ Å, crossed Goebel mirrors) and phi and omega scans.[20] The data reduction was performed by using the program SAINT+.[21] The empirical absorption corrections were performed by using SADABS.[22] The structures were solved by using direct methods with SHELXS-97 and refined by using full-matrix least-squares methods based on F^2 by using SHELXS-97.[23] The single-crystal X-ray diffraction data for **4a** were collected by using an Oxford Diffraction SuperNova diffractometer equipped with an Eos CCD detector and MoK_α radiation, $\lambda = 0.71073$ Å. Data frames were processed (unit cell determination, intensity data integration, correction for Lorentz and polarisation effects, and empirical absorption correction) by using the corresponding diffractometer's software package.[24]

The program MERCURY was used to prepare molecular graphic images.[25] All non-hydrogen atoms were refined anisotropically, and the hydrogen atoms were placed in calculated positions with displacement factors fixed at $1.2\times U_{eq}$ of the parent C atoms or $1.5\times U_{eq}$ for methyl groups.

The site occupancy factors of the disordered THF molecules (modelled over two positions) that fill the channels around the fourfold screw axis in **4** were fixed at 0.125, a value that agrees with the result from the TGA performed at the same time as the data collection (Figure S7 in the Supporting Information). Restraints were placed on some of the bond lengths and the anisotropic displacement parameters of the disordered THF molecule.

The crystal of **4a** was found to be non-merohedrally twinned. The HKLF 4 format file (with the non-overlapping reflections of component one only) was used to solve the structure. The HKLF 5 format file was used for the refinement of the structure, BASF 0.502(2). Restraints were placed on the anisotropic displacement parameters of C8 and C13. In compound **5**, restraints were placed on some of the bond lengths and the anisotropic displacement parameters of the disordered *tert*-butyl groups that contained C10 and C26. CCDC 1412128 (■■compound #?■■), 1412129 (■■) and 1412130 (■■) contain the supplementary crystallographic data for this paper. These data are provided free of charge by The Cambridge Crystallographic Data Centre.

Crystal Data for 4

$C_{52}H_{72}O_4Se_8{\cdot}C_4H_8O$; $M_r = 1464.88$; colourless block; tetragonal; space group $P4_2/n$ (No. 86); $a = b = 17.9571(4)$, $c = 10.1875(5)$ Å; $V =$ 3285.03(19) Å^3; $Z = 2$; $\rho_{calcd} = 1.481$ g cm^{-3}; $F_{000} = 1456$; $T = 100(2)$ K; $2\theta_{max} = 140.5°$; 231112 reflections collected, 3086 unique ($R_{int} =$ 0.1005). Final GOF = 1.143; $R_1 = 0.0721$, $wR_2 = 0.1628$, R indices based on 2374 reflections with $I > 2\sigma(I)$ (refinement on F^2), 224 parameters, 94 restraints. Lp and absorption corrections applied, $\mu =$ 5.516 mm^{-1}.

Crystal Data for 4a

$C_{52}H_{72}O_4Se_8$; $M_r = 1392.78$; yellowish block; triclinic; space group $P1$ (No. 2); $a = 9.557(3)$, $b = 10.453(2)$, $c = 14.025(4)$ Å; $\alpha = 103.54(2)$, $\beta = 98.56(2)$, $\gamma = 90.38(2)°$; $V = 1345.7(6)$ Å^3; $Z = 1$; $\rho_{calcd} =$ 1.719 g cm^{-3}; $F_{000} = 688$; $T = 100(2)$ K; $2\theta_{max} = 50.7°$; 7245 reflections collected, 7280 unique. Final GOF = 0.843; $R_1 = 0.0944$, $wR_2 =$ 0.2373, R indices based on 2330 reflections with $I > 2\sigma(I)$ (refine-

ment on F^2), 299 parameters, 12 restraints. Lp and absorption corrections applied, $\mu = 5.473$ mm^{-1}.

Crystal data for 5

$C_{56}H_{80}O_4Se_8 \cdot 2C_4H_8O$; $M_r = 1593.09$; colourless plate; monoclinic; space group $C2/c$ (No. 15); $a = 35.6317(12)$, $b = 10.2606(3)$, $c = 25.3919(9)$ Å; $\beta = 133.465(2)^\circ$; $V = 6737.8(4)$ Å^3; $Z = 4$; $\rho_{calcd} = 1.570$ g cm^{-3}; $F_{000} = 3200$; $T = 100(2)$ K; $2\theta_{max} = 143.5^\circ$; 32 180 reflections collected, 6186 unique ($R_{int} = 0.0818$). Final GOF = 1.022; $R_1 = 0.0479$, $wR_2 = 0.1124$, R indices based on 4929 reflections with $I > 2\sigma(I)$ (refinement on F^2), 422 parameters, 29 restraints. Lp and absorption corrections applied, $\mu = 5.440$ mm^{-1}.

Molecular Modelling Studies

The structures corresponding to the homodiselenacalix[4]arene macrocycles with three, four and five subunits were constructed by using the Marvin software provided by ChemAxon,[26] with the structures being further optimised by applying an AM1 semi-empirical method as implemented in the Gaussian 03 software.[27] The optimised structure was further refined by means of ab initio methods, in which the corresponding electronic structure and electrostatic potential was calculated.

For the molecular dynamics studies the AMBER12 software package was used.[28] The structure corresponding to macrocycle **4** was parameterised by using the GAFF■■please define■■ force field,[29] with the corresponding charges being derived from the above-mentioned ab initio calculations by applying the restrained electrostatic potential (RESP) fitted charges method. Missing atomic parameters in the GAFF force fields for Se atoms were manually added (i.e., mass, polarisability and Se–Se bonds), whereas standard and dihedral angles that involved Se atoms were assumed to be identical to those already parameterised for sulfur within the GAFF force field.

MD trajectories obtained under implicit solvent conditions were performed by considering the dielectric constant reported for THF (i.e., 7.6). The systems simulated under these conditions were initially minimised (10 000 steps), after which a heating phase was applied to gradually equilibrate the systems from 0 to 300 K over 1.2 ns with a 1 fs timestep. After the system temperature was equilibrated, a production phase was applied to obtain a 10 ns trajectory, from which the corresponding energetic components were analysed.

MD trajectories obtained under explicit solvent conditions were performed by using a solvent system developed in-house. Initially, one molecule of THF was modelled, with its electronic properties being determined by using ab initio methods as implemented in the Gaussian 03 software.[27] To generate an initial box of 30 Å^3 that contained the modelled THF molecules, the Packmol software was used,[30] with this box being then equilibrated at 300 K by using standard MD simulations. The density of the solvent box was used as a quality check, and after reaching the target reported density (0.889 g mL^{-1}), the box was saved and applied to the following MD explicit solvent runs. For MD simulations of the homodiselenacalix[*n*]arene macrocycles, the corresponding molecules were solvated by using an octahedral THF box, after which an initial minimisation of the solvent followed by a minimisation of the whole system was carried out. The minimised systems were progressively heated to 300 K over 50 ps, followed by a 100 ps equilibration run. Production runs intended for analyses were performed for 10 ns with a 2 fs timestep and under constant pressure and temperature conditions, with the SHAKE algorithm being applied to constrain bonds that involved hydrogens.

Trajectory properties were processed and analysed by using the cpptraj module of AMBER12.[28■ok?■] The structures analysed and images presented were prepared by using the VMD v.1.8.6 software.[31] MD trajectories were obtained by using CUDA-designed code (pmemd.cuda), with computational facilities provided by the GPGPU Computing group at the Facultad de Matemática, Astronomía y Física (FAMAF), Universidad Nacional de Córdoba, Argentina.

Acknowledgements

We thank the Fonds Wetenschappelijk Onderzoek (FWO), the KU Leuven, Hasselt University and BELSPO (IAP 7/05 FS2) for financial support, and the Hercules Foundation for supporting the purchase of a diffractometer through project AKUL/09/0035. We would also like to acknowledge Dr. Grażyna Szczepańska for the TGA analysis. M.A.Q. acknowledges financial support from the Secretaría de Ciencia y Técnica of the Universidad Nacional de Córdoba (SECyT-UNC) and the Consejo Nacional de Investigaciones Científicas y Técnicas (CONICET). M.A.Q. also acknowledges the GPGPU Computing Group and Dr. Nicolás Wolovick from the Facultad de Matemática, Astronomía y Física (FAMAF), Universidad Nacional de Córdoba, Argentina, for providing access to computing resources.

Keywords: calixarenes · covalent chemistry · crystal engineering · molecular dynamics · selenium

[1] a) K. Kobayashi, M. Yamanaka, *Chem. Soc. Rev.* **2015**, *44*, 449; b) P. Sozzani, S. Bracco, A. Comotti, L. Ferretti, R. Simonutti, *Angew. Chem. Int. Ed.* **2005**, *44*, 1816; *Angew. Chem.* **2005**, *117*, 1850; c) S. Lim, K. Hyunuk, S. Narayanan, K. Kyung-Jin, C. J. Sung, S. Gon, K. Kimoon, *Angew. Chem. Int. Ed.* **2008**, *47*, 3352; *Angew. Chem.* **2008**, *120*, 3400; d) L. S. Shimizu, S. R. Salpage, A. A. Korous, *Acc. Chem. Res.* **2014**, *47*, 2116; e) R. Gleiter, D. B. Werz, B. J. Rausch, *Chem. Eur. J.* **2003**, *9*, 2676; f) A. Comotti, S. Bracco, G. Distefano, P. Sozzani, *Chem. Commun.* **2009**, 284.

[2] a) S. Horike, S. Shimomura, S. Kitagawa, *Nat. Chem.* **2009**, *1*, 695; b) D. Bradshaw, J. B. Claridge, E. J. Cussen, T. J. Prior, M. J. Rosseinsky, *Acc. Chem. Res.* **2005**, *38*, 273.

[3] a) M. Miyata, M. Shibakami, S. Chirachanchai, K. Takemoto, N. Kasai, K. Miki, *Nature* **1990**, *343*, 446; b) J. T. A. Jones, D. Holden, T. Mitra, T. Hassel, D. J. Adams, K. E. Jelfs, A. Trevin, D. J. Willock, G. M. Day, J. Bacsa, A. Steiner, A. I. Cooper, *Angew. Chem. Int. Ed.* **2011**, *50*, 749; *Angew. Chem.* **2011**, *123*, 775; c) C. Massera, M. Melegari, E. Kalenius, F. Ugozzoli, E. Dalcanale, *Chem. Eur. J.* **2011**, *17*, 3064.

[4] For homodithiacalixarenes, see: a) J. Thomas, G. Reekmans, P. Adriaensens, L. Van Meervelt, M. Smet, W. Maes, W. Dehaen, L. Dobrzańska, *Angew. Chem. Int. Ed.* **2013**, *52*, 10237; *Angew. Chem.* **2013**, *125*, 10427; b) J. Thomas, L. Dobrzańska, M. P. Sonawane, W. Maes, M. Smet, W. Dehaen, *Supramol. Chem.* **2014**, *26*, 591.

[5] a) J. L. Atwood, L. J. Barbour, A. Jerga, *Science* **2002**, *296*, 2367; b) G. S. Ananchenko, I. L. Moudrakovski, A. W. Coleman, J. A. Ripmeester, *Angew. Chem. Int. Ed.* **2008**, *47*, 5616; *Angew. Chem.* **2008**, *120*, 5698; c) P. K. Thallapally, B. P. McGrail, S. J. Dalgarno, H. T. Schaef, J. Tian, J. L. Atwood, *Nat. Mater.* **2008**, *7*, 146; d) P. K. Thallapally, B. P. McGrail, J. L. Atwood, C. Gaeta, C. Tedesco, P. Neri, *Chem. Mater.* **2007**, *19*, 3355; e) S. J. Dalgarno, J. Tian, J. E. Warren, T. E. Clark, M. Makha, C. L. Raston, J. L. Atwood, *Chem. Commun.* **2007**, 4848.

[6] For heteracalix[*n*]arenes, see: a) P. Lhoták, *Eur. J. Org. Chem.* **2004**, 1675; b) N. Morohashi, F. Narumi, N. Iki, T. Hattori, S. Miyano, *Chem. Rev.* **2006**, *106*, 5291; c) W. Maes, W. Dehaen, *Chem. Soc. Rev.* **2008**, *37*, 2393; d) M.-

X. Wang, *Chem. Commun.* **2008**, 4541; e) M.-X. Wang, *Acc. Chem. Res.* **2012**, *45*, 182.

[7] a) W. Maes, W. Van Rossom, K. Van Hecke, L. Van Meervelt, W. Dehaen, *Org. Lett.* **2006**, *8*, 4161; b) W. Van Rossom, W. Maes, L. Kishore, M. Ovaere, L. Van Meervelt, W. Dehaen, *Org. Lett.* **2008**, *10*, 585; c) W. Van Rossom, M. Ovaere, L. Van Meervelt, W. Dehaen, W. Maes, *Org. Lett.* **2009**, *11*, 1681; d) J. Thomas, W. Van Rossom, K. Van Hecke, L. Van Meervelt, M. Smet, W. Maes, W. Dehaen, *Chem. Commun.* **2012**, *48*, 43; e) W. Van Rossom, J. Caers, K. Robeyns, L. Van Meervelt, W. Maes, W. Dehaen, *J. Org. Chem.* **2012**, *77*, 2791; f) W. Van Rossom, J. Thomas, T. G. Terentyeva, W. Maes, W. Dehaen, *Eur. J. Org. Chem.* **2013**, 2085; g) J. Thomas, W. Van Rossom, K. Van Hecke, L. Van Meervelt, M. Smet, W. Maes, W. Dehaen, *Synthesis* **2013**, *45*, 2085.

[8] For homocalix[*n*]arenes, see: a) S. Ibach, V. Prautzsch, F. Vogtle, *Acc. Chem. Res.* **1999**, *32*, 729; b) A. V. Predeus, V. Gopalsamuthiram, R. J. Staples, W. D. Wulff, *Angew. Chem. Int. Ed.* **2013**, *52*, 911; *Angew. Chem.* **2013**, *125*, 945.

[9] For homooxacalixarenes, see: a) B. Masci, M. Finelli, M. Varrone, *Chem. Eur. J.* **1998**, *4*, 2018; b) E. A. Shokova, V. V. Kovalev, *Russ. J. Org. Chem.* **2004**, *40*, 607; c) E. A. Shokova, V. V. Kovalev, *Russ. J. Org. Chem.* **2004**, *40*, 1547; d) K. Cottet, P. M. Marcos, P. J. Cragg, *Beilstein J. Org. Chem.* **2012**, *8*, 201.

[10] For homoazacalixarenes, see: a) K. Ito, M. Noike, A. Kida, Y. Ohba, *J. Org. Chem.* **2002**, *67*, 7519; b) C. Kaewtong, S. Fuangswasdi, N. Muangsin, N. Chaichit, J. Vicens, B. Pulpoka, *Org. Lett.* **2006**, *8*, 1561; c) C. Kaewtong, G. Jiang, Y. Park, T. Fulghum, A. Baba, B. Pulpoka, R. Advincula, *Chem. Mater.* **2008**, *20*, 4915; d) M. Arunachalam, I. Ravikumar, P. Ghosh, *J. Org. Chem.* **2008**, *73*, 9144; e) H. Takemura, Y. Yonebayashi, T. Nakagaki, T. Shinmyozu, *Eur. J. Org. Chem.* **2011**, 1968.

[11] For homothiacalixarenes, see: a) J. Thomas, K. Van Hecke, K. Robeyns, W. Van Rossom, M. P. Sonawane, L. Van Meervelt, M. Smet, W. Maes, W. Dehaen, *Chem. Eur. J.* **2011**, *17*, 10339; b) M. P. Sonawane, K. Van Hecke, J. Jacobs, J. Thomas, L. Van Meervelt, W. Dehaen, W. Van Rossom, *J. Org. Chem.* **2012**, *77*, 8444; c) M. Hučko, H. Dvořàkovà, V. Eigner, P. Lhotàk, *Chem. Commun.* **2015**, *51*, 7051.

[12] For homoselenacalixarenes, see: a) J. Thomas, W. Maes, K. Robeyns, M. Ovaere, L. Van Meervelt, M. Smet, W. Dehaen, *Org. Lett.* **2009**, *11*, 3040; b) J. Thomas, L. Dobrzańska, K. Van Hecke, M. P. Sonawane, K. Robeyns, L. Van Meervelt, K. Woźniak, M. Smet, W. Maes, W. Dehaen, *Org. Biomol. Chem.* **2012**, *10*, 6526.

[13] a) S. J. Rowan, S. J. Cantrill, G. R. L. Cousins, J. K. M. Sanders, J. F. Stoddart, *Angew. Chem. Int. Ed.* **2002**, *41*, 898; *Angew. Chem.* **2002**, *114*, 938; b) P. T. Corbett, J. Leclaire, L. Vial, K. R. West, J. L. Wietor, J. K. M. Sanders, S. Otto, *Chem. Rev.* **2006**, *106*, 3652; c) S. P. Black, J. K. M. Sanders, A. R. Stefankiewicz, *Chem. Soc. Rev.* **2014**, *43*, 1861.

[14] a) W. Cao, X. Zhang, X. Miao, Z. Yang, H. Xu, *Angew. Chem. Int. Ed.* **2013**, *52*, 6233; *Angew. Chem.* **2013**, *125*, 6353; b) S. Ji, W. Cao, Y. Yu, H. Xu, *Angew. Chem. Int. Ed.* **2014**, *53*, 6781; *Angew. Chem.* **2014**, *126*, 6899■ ■changed to match records; ok?■■; c) B. Rasmussen, A. Sørensen, H. Gotfredsen, M. Pittelkow, *Chem. Commun.* **2014**, *50*, 3716.

[15] a) K. P. Bhabak, G. Mugesh, *Acc. Chem. Res.* **2010**, *43*, 1408; b) H. Xu, W. Cao, X. Zhang, *Acc. Chem. Res.* **2013**, *46*, 1647; c) X. Miao, W. Cao, W. Zheng, J. Wang, X. Zhang, J. Gao, C. Yang, D. Kong, H. Xu, L. Wang, Z. Yang, *Angew. Chem. Int. Ed.* **2013**, *52*, 7781; *Angew. Chem.* **2013**, *125*, 7935.

[16] D. Manna, G. Roy, G. Mugesh, *Acc. Chem. Res.* **2013**, ***46***, 2706.

[17] a) W. Cao, Y. Li, Y. Yi, S. Ji, L. Zeng, Z. Sun, H. Xu, *Chem. Sci.* **2012**, *3*, 3403; b) X. Miao, W. Cao, W. Zheng, J. Wang, X. Zhang, J. Gao, C. Yang, D. Kong, H. Xu, L. Wang, Z. Yang, *Angew. Chem. Int. Ed.* **2013**, *52*, 7781; *Angew. Chem.* **2013**, *125*, 7935.■■duplicate of [15c]; please remove/replace one & renumber■■

[18] a) A. Panda, *Coord. Chem. Rev.* **2009**, *253*, 1056; b) A. J. Mukherjee, S. S. Zade, H. B. Singh, R. B. Sunoj, *Chem. Rev.* **2010**, *110*, 4357; c) P. Kumar, V. S. Kashid, J. T. Mague, M. S. M. Balakrishna, *Tetrahedron Lett.* **2014**, *55*, 5232.

[19] Upon further examination of the system, it was noted that the transformation works best immediately after crystallisation, by using fresh material (TGA and XRPD were performed on fresh material). After a couple of days, the crystal start to become yellowish and then turn orange (Figure S2 in the Supporting Information). The single-crystal XRD data collection performed on an orange crystal indicates replacement of THF molecules by water molecules, which takes place over the course of a couple of days if the crystals are not being stored in sealed capillaries or under an inert atmosphere. This replacement, however, does not cause bigger changes in the crystal structure, nor in the unit cell parameters ($a=b=17.9276(8)$, $c=10.1770(4)$ Å, $V=3270.8(3)$ Å^3). In the case of the disulfide analogue, this change also takes place but requires months to occur. We have also noticed that removal of the water molecules is possible and is connected with a conformational change, but the crystals need to be heated for a longer time at higher temperatures ($\approx 160\,^{\circ}$C).

[20] SMART (version 5.628), Data collection software, Bruker Analytical X-ray Instruments Inc., Madison, Wisconsin (USA) **2002**.

[21] SAINT+ (version 6.45), Data reduction software, Bruker Analytical X-ray Instruments Inc., Madison, Wisconsin (USA) **2003**.

[22] G. M. Sheldrick, SADABS (version 2.03), Program for Empirical Absorption Correction of Area Detector Data, University of Göttingen, Göttingen (Germany) **2002**.

[23] G. M. Sheldrick, *Acta Crystallogr. A* **2008**, *64*, 112.

[24] CrysAlisPro CCD and RED, version 1.171.35.21, Oxford Diffraction, Ltd., Oxford, U. K., **2012**.

[25] C. F. Macrae, I. J. Bruno, J. A. Chisholm, P. R. Edgington, P. McCabe, E. Pidcock, L. Rodriguez-Monge, R. Taylor, J. van de Streek, P. A. Wood, *J. Appl. Crystallogr.* **2008**, *41*, 466.

[26] MarvinSketch v.6.31., ChemAxon Ltd.

[27] Gaussian 03, Revision C.02, M. J. Frisch, G. W. Trucks, H. B. Schlegel, G. E. Scuseria, M. A. Rob, J. R. Cheeseman, J. A. Montgomery Jr., T. Vreven, K. N. Kudin, J. C. Burant, J. M. Millam, S. S. Iyengar, J. Tomasi, V. Barone, B. Mennucci, M. Cossi, G. Scalmani, N. Rega, G. A. Petersson, H. Nakatsuji, M. Hada, M. Ehara, K. Toyota, R. Fukuda, J. Hasegawa, M. Ishida, T. Nakajima, Y. Honda, O. Kitao, H. Nakai, M. Klene, X. Li, J. E. Knox, H. P. Hratchian, J. B. Cross, V. Bakken, C. Adamo, J. Jaramillo, R. Gomperts, R. E. Stratmann, O. Yazyev, A. J. Austin, R. Cammi, C. Pomelli, J. W. Ochterski, P. Y. Ayala, K. Morokuma, G. A. Voth, P. Salvador, J. J. Dannenberg, V. G. Zakrzewski, S. Dapprich, A. D. Daniels, M. C. Strain, O. Farkas, D. K. Malick, D. K. Rabuck, K. Raghavachari, J. B. Foresman, J. V. Ortiz, Q. Cui, A. G. Baboul, S. Clifford, J. Cioslowski, B. B. Stefanov, G. Liu, A. Liashenko, P. Piskorz, I. Komaromi, R. L. Martin, D. J. Fox, T. Keith, M. A. Al-Laham, C. Y. Peng, A. Nanayakkara, M. Challacombe, P. M. W. Gill, B. Johnson, W. Chen, M. W. Wong, C. Gonzalez, J. A. Pople, Gaussian, Inc., Wallingford CT, **2004**.

[28] R. Salomon-Ferrer, D. A. Case, R. C. Walker, *WIREs* **2013**, *3*, 198.

[29] J. Wang, R. M. Wolf, J. W. Caldwell, P. A. Kollman, D. A. Case, *J. Comput. Chem.* **2004**, *25*, 1157.

[30] L. Martinez, R. Andrade, E. G. Birgin, J. M. Martínez, *J. Comput. Chem.* **2009**, *30*, 2157.

[31] W. Humphrey, A. Dalke, K. Schulten, *J. Mol. Graph.* **1996**, *14*, 33.

Received: August 26, 2015
Published online on ■■ ▮▮, 0000

FULL PAPER

Macrocycles

*J. Thomas, L. Dobrzańska, L. Van Meervelt, M. A. Quevedo, K. Woźniak, M. Stachowicz, M. Smet, W. Maes, W. Dehaen**

■■ – ■■

Homodiselenacalix[4]arenes: Molecules with Unique Channelled Crystal Structures

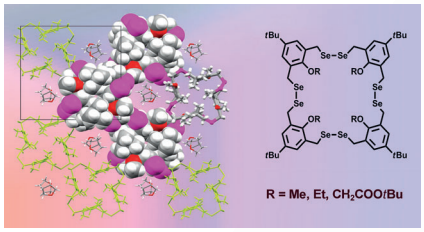

Change the channel: A new family of calixarene macrocycles, homodiselenacalix[4]arenes (see figure), were prepared by applying the dynamic covalent chemistry of diselenide bonds. In the single crystal, the calixarene molecules can switch between two conformations in a concerted fashion as a response to the right external stimuli.

Please check that the ORCID identifiers listed below are correct. We encourage all authors to provide an ORCID identifier for each coauthor. ORCID is a registry that provides researchers with a unique digital identifier. Some funding agencies recommend or even require the inclusion of ORCID IDs in all published articles, and authors should consult their funding agency guidelines for details. Registration is easy and free; for further information, see http://orcid.org/.

Dr. Joice Thomas
Dr. Liliana Dobrzańska
Prof. Luc Van Meervelt
Prof. Mario Alfredo Quevedo
Krzysztof Woźniak
Marcin Stachowicz
Prof. Mario Smet
Prof. Wouter Maes
Prof. Wim Dehaen